ISSN 1330-3651 (Print), ISSN 1848-6339 (Online) https://doi.org/10.17559/TV-20250420002612
Original scientific paper

Study on Impact Effect of Curved Steel-Mixed Composite Beam Bridge Based on Coupling Vibration of Vehicle-Bridge

Hao QU*, Yufeng LIU, Shuigen HU

Abstract: Based on the detailed study of the domestic and foreign standardized impact coefficient regulations and the collection of a large number of bridge sports car test data, this paper uses the ABAQUS finite element model to establish the axial coupling vibration analysis model. Considering that the upper structure of the curved bridge is affected by the coupling of bending and torsion under the action of the vehicle, the finite element software ANSYS and Dynamics software UM are used to analyze and study the spanning response of the curved bridge under the coupling effect of the axle. In response to the influence of heavy vehicles on steel composite girder Bridges, this paper compares and analyzes the influence of factors such as vehicle speed, vehicle weight and unstable bridge deck on the displacement influence coefficient and bending moment influence coefficient, and compares the difference with the standard calculated influence coefficient. The results show that the influence of vehicle speed on the impact coefficient increases first and then decreases, and the maximum value is reached at 80 km/h. The impact coefficient is greatly affected by road roughness, and increases with the decrease of road grade. The impact coefficient decreases with the increase of vehicle weight. The damping of vehicle (suspension system and tire) has little influence on the impact coefficient, which can be ignored in the study. The relationship between vehicle driving radius and impact coefficient is complicated. The impact coefficient of lateral deflection reaches the maximum value at the center line of the bridge, the impact coefficient of vertical deflection presents positive symmetry, and the impact coefficient of bending moment presents an antisymmetric trend, and the impact coefficient of torque is more sensitive to the vehicle driving radius.

Keywords: axle coupling vibration; dynamic load test; factors of irregularity; impact coefficient; steel-composite beam bridge

1 INTRODUCTION

The vibration of the bridge will be induced by the vehicle's passage through it, and the vibration of the vehicle will be influenced by the vibration of the bridge. The coupling vibration problem of the vehicle and the bridge is the term used to describe the issue of mutual influence between the two. When the vehicle passes over the bridge, it is often greater than the effect on the bridge under static load, and the ratio of the two is defined as the impact coefficient. The curved steel-concrete composite continuous bridge has the advantages of low dead weight, high stiffness, fast construction speed, etc., and can well adapt to the requirements of terrain and line, so it is widely used in urban viaduct, river crossing and other lines [1]. With the increase of vehicles, the impact load exerted by vehicles on the bridge gradually increases, which has a certain impact on the beam structure [2]. Compared with general linear Bridges, curved Bridges are more susceptible to flexural and torsional coupling [3, 4], and their forces are more complex. Therefore, it is of great engineering significance to study the dynamic response of the bridge superstructure of curved steel-concrete composite continuous Bridges under vehicle-bridge coupling.

Steel-concrete composite beam bridge is a bridge structure composed of steel beams and concrete bridge panels, which are combined together by shear connectors [5]. In many cases, steel-concrete composite beam bridge has good comprehensive technical and economic benefits and social benefits. Compared with concrete bridge, it has the characteristics of lower superstructure height, light dead weight and less earthquake action. Steel-mixed composite beam bridge is also convenient for factory production and has the advantage of fast construction, which can reduce the project cost [6]. Due to the vehicle-bridge coupling effect, vehicles will have a certain impact on the bridge while driving, and the dynamic response generated can be significantly higher than the response caused by static load [7].

Currently, the investigation of vehicle-bridge coupling vibration is primarily focused on linear bridges, while the investigation of curved bridges is less prevalent. Consequently, this paper establishes a refined finite element model of a curved steel-concrete composite continuous beam bridge, and its multi-rigid body vibration model is established in accordance with an actual vehicle. The dynamic model of the vehicle and curvilinear bridge coupling is established to enable the vehicle to operate on the curve lane under a variety of working conditions, utilizing the fundamental principle of the mode superposition method. The superstructure of a curved steel-concrete composite continuous beam is analyzed in relation to the influence of vehicle speed, road irregularity, and partial load. This analysis serves as a reference for the design and maintenance of bridges of the same type. The first part of this article is an introduction, and the second part is an introduction to the relevant work. The third part is analysis of influencing factors of coupling vibration response of steel-mixed composite beam bridge. The fourth part is the comparative study on impact coefficient of curved steel-hybrid continuous beam bridge, and the fifth part is the conclusion.

2 RELATED WORK

There is a wealth of theoretical groundwork for bridge study and design provided by the bridge response acquired through vehicle-bridge coupling. The simulation results are consistent with the lateral force coefficient in the "General Code for Design of Highway Bridges and Culverts" (JTG D60-2015). However, the simulation calculation of the three-span continuous steel structure bridge under vehicle load was carried out, and the impact effect was not considered. A frequently utilized method for studying vehicle-bridge interaction dynamics, the modal superposition approach, considerably enhances computing efficiency [6]. In literature [7], the displacement, bending moment and shear impact coefficient of long-span curved beam Bridges and their relationships were theoretically

predicted, and the theoretical results were verified by the 7-DOF vehicle model and the curvilinear beam model. By establishing a vehicle-deck pavement coupling model [8], the influences of single-vehicle, multi-vehicle and off-load conditions on bridge deck response were explored, and the vehicle-bridge coupling in the macro world was creatively linked to the tire-road contact relationship in the micro world. The research target is a three-span continuous box girder bridge. To study and assess the impact coefficient of the bridge structure under vehicle load, a vehicle-bridge coupling dynamic model is formed by establishing a bridge model and a vehicle model [9].

In recent years, curved continuous girder Bridges have been widely used in expressway cross-line interworking, long-span bridge approach and urban interchange. The static theory of curved beam bridge structure has been well developed in recent decades, but the dynamic effect still needs further study according to the coordination conditions of contact force and displacement of contact points changing with time between vehicle-curve bridge systems [10]. A three-span curved continuous beam bridge was analyzed using a 15-degree-of-freedom vehicle model that was established using the modal synthesis approach [11]. In order to study how the speed of the vehicle and the curvature radius of the deck irregularity affect the dynamic response of the curved beam bridge, the vehicle-bridge coupling vibration analysis module was built using the MATLAB program. This study examines the effects of vehicle load on bridge deflection and the radius of curvature on torsion of curved bridges. The structural dynamic response [12] was solved using Newmark-β. The dynamic response analysis program of curved beam bridge was developed based on MATLAB platform, and the corresponding simulation program of road roughness based on Fourier transform was written, and the bridge response results calculated by ANSYS software were compared. A vehicle-bridge coupling dynamic response analysis was carried out on a five-span concrete continuous beam [13], which completed the modeling and analysis of the bridge and 23-DOF vehicle under ANSYS environment. The analysis results of the beam element and the solid element were compared, and the solid element's response results were higher and safer. On this basis, the effects of geometric nonlinearity and material nonlinearity on the response were considered, and the off-load, vehicle speed and centrifugal force were analyzed. In addition, on the basis of this research, a driver model with nonlinear delay is inserted into the vehicle model [14] to calculate the appropriate steering angle of the front wheels of the vehicle, so that the vehicle can drive according to the prescribed route. This application makes the vehicle-bridge coupling research of curved bridges more accurate. Based on UM multi-body dynamic simulation software, the vehicle-bridge coupling simulation was carried out on a four-span curved continuous concrete beam [15], the stress of asphalt layer under vehicle load was analyzed, and the analysis results were verified by dynamic and static load test. The causes of the diseases such as enveloping and cracking of pavement layer were given, and the dynamic response of vehicles under various working conditions was solved.

The modal superposition method is proposed in literature [16]. By converting the bridge response from physical space to modal space, satisfactory accuracy can be obtained by taking only a few low-order states, which greatly improves the computational efficiency, and has been widely used in the study of vehicle-bridge coupling dynamics. For the overall response of the bridge, only a few low-order modes can be used to calculate the satisfactory results. For the local response, due to the influence of the bridge higher-order mode, the order of the superposition mode should be appropriately increased in the calculation [17]. The modal synthesis method is suitable for linear vehicle-bridge coupling problems, but it is powerless for Bridges considering material nonlinearity and linear nonlinearity. As the latest multi-body dynamics software, UM has been widely favored by scholars in recent years due to its unique solution method PARK integral method, which makes the solution speed faster than the traditional solution of modal synthesis method, and its convenient vehicle modeling method. Program for multi-body dynamics, the concrete-filled steel tube arch bridge's vehicle-bridge coupling resonance system is studied using UM [18]. In order to create the same frequency resonance effect, the truncated bridge's frequency is comparable to the vehicle's. Using UM as a foundation, a 9-degree-of-freedom vehicle model was developed to examine both continuous box girder bridges with corrugated steel webs and continuous beam bridges with concrete webs [19]. Researchers observed that coupling vibration was more noticeable in continuous rigid frame bridges with corrugated steel webs compared to those with concrete webs.

This paper studies the problem of driving comfort under the influence of vehicle-bridge coupling vibration [20], and the analysis shows that driving comfort deteriorates with the increase of vehicle speed. In this research process, the 9-DOF spatial vehicle model is used, combined with the three-dimensional model of long-span highway cable-stayed bridge, and the weighted acceleration of vehicles is taken as the evaluation index. In order to assess the extent of foundation damage, we modelled the wave load that can induce vibrations in the vehicle-bridge lateral coupling [21], investigated the effects of such a wave on the bridge's base, and ultimately determined the level of vibration in the vehicle and its dynamic reaction to the wave. We studied the vehicle-induced vibration response of the bridge using the coupled vehicle-bridge-foundation vibration model [22]. By examining the frequency and mode of the bridge dynamic response, we were able to quantify the degree of erosion to the foundation. A number of studies were carried out on model building, vibration analysis, impact coefficient, and scaled model test, all based on the virtual excitation method [23]. The vibration of the vehicle-bridge coupling of the highway beam bridge was examined under the condition of non-stationary random input of the road irregularity spectrum. An analysis of the reinforcing impact of reinforced concrete tied arch bridge was conducted using the study results of vehicle-bridge coupling vibration [24]. The vibration mechanism of the vehicle-bridge coupling and the parameters that influence it in a double-I-beam steel-concrete slab composite beam bridge are investigated using numerical simulation [25] and data collected from actual measurements. A technique for analyzing vibrations between vehicles and bridges was suggested [26].

In summary, with the development of theory and the improvement of test technology, the research of vehicle-bridge coupling vibration has been developed in the direction of practical refinement. Among them, the selection of vehicle model has experienced the evolution process from simple to complex, from plane to space. In the research process of many scholars, the bridge models are generally simple supported beams and continuous beams, etc., and the research on the coupling vibration of the vehicle-bridge of steel-mixed composite beam bridge is less. Therefore, the coupling vibration of vehicle-bridge is studied in this paper.

3 ANALYSIS OF INFLUENCING FACTORS OF COUPLING VIBRATION RESPONSE OF STEEL-MIXED COMPOSITE BEAM BRIDGE

3.1 Analysis of Dynamic Characteristics of Steel-Composite Beam Bridge

A newly built steel-mixed composite beam bridge is a demolition and reconstruction project. The calculated span of the bridge is 105 m, and the span arrangement is 3 × 35 m. The bridge pier adopts column pier, the abutment adopts one-line platform, and the foundation is bored pile. The design vehicle load grade is city-A, the road grade is the main road of the city, and the design running speed is 60 km/h.

The bridge layout is shown in Fig. 1.

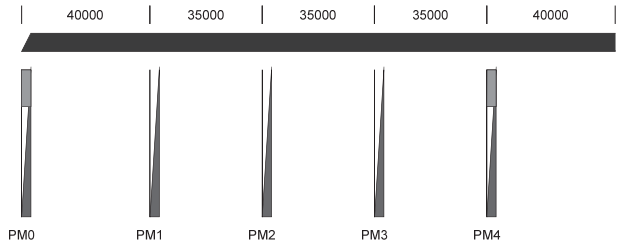

Figure 1 Bridge layout (Unit: mm)

The upper structure of the bridge adopts three span double I-beam and concrete slab continuous composite beam bridge. The type of bridge support is friction swing support, and the expansion joint adopts comb type expansion joint. The bridge deck is arranged according to the two-way 4 lanes, and the double full width is 24 m.

The variable definitions used in the text are shown in Tab. 1.

Table 1 Variable definition

Variable	Definition
F_z	normal force
z_0	bridge floor irregularity
z_t	vertical displacement of the tire
z_b	displacement of the bridge floor and the contact position of the tire
d_z	tire damping
h	vertical deformation rate of the tire
F_x	tire longitudinal force
F_y	Tire lateral force
r_t	tire radius,

The English abbreviations are shown in Tab. 2.

Tab. 3 shows that the steel-hybrid composite beam bridge has a mode characteristic of vertical antisymmetric bending and a fundamental frequency of 2.7197 Hz. Because the bridge's vertical stiffness is lower than its lateral stiffness, the initial transverse bending happens in the eighth vibration mode, after three modes that are characterized by vertical bending. In the initial 10 vibration modes, four of them are torsional, suggesting that the bridge has a low torsional stiffness and would exhibit a torsional trend when subjected to vehicle loads, which in turn increases the vibration effect. It is imperative that the appropriate authorities enhance their methods for identifying these bridges and determining their carrying capability.

Table 2 Abbreviations

Abbreviations	Full name
UM	User Manual
RGD	Reacting Gas Dynamics
ABAQUS	Advanced Simulation for Engineering and Sciences

Table 3 First 10 natural vibration frequency and vibration mode characteristics of steel-mixed composite beam bridge

Rank	Frequency / Hz	Mode description	Rank	Frequency / Hz	Mode description
1	2.7197	Vertical first order bending	6	7.3325	Vertical fourth order bending
2	3.6167	Vertical second-order bending	7	7.8840	Third order torsion
3	3.6885	Vertical third order bending	8	8.6781	Transverse first order bending
4	5.5481	Torsion of first order	9	8.7859	Fourth order torsion
5	7.3001	Second order torsion	10	9.1985	Vertical fifth order bending

Fig. 2 shows the results of the spatial finite element model of a 3 × 35 m steel-mixed composite beam bridge half-width that was created using ANSYS software in this work. Using the Solid65 unit to simulate the bridge's concrete material, the Beam189 unit to model the steel main and cross beams, a rigid arm to join the steel beams to the bridge panel, and the constraint mode of a continuous beam bridge to impose boundary conditions.

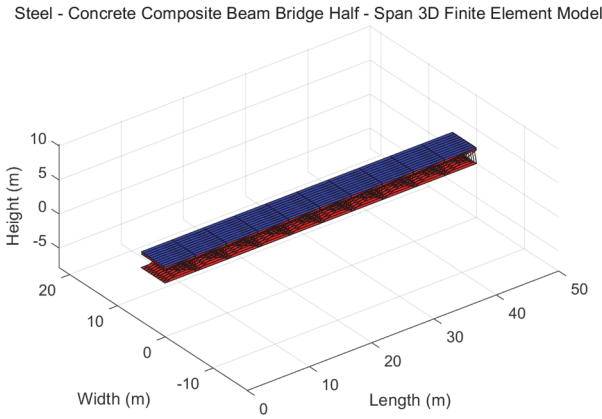

Figure 2 Finite element model of half-width bridge of steel-mixed composite beam bridge

3.2 Analysis of Influencing Factors of Bridge Dynamic Response

The contact relationship between tire and bridge deck pavement is the key to connect the two subsystems of

vehicle and bridge. The RGD tire model based on elastic foundation beam theory is selected. The normal force of tire path contact depends on the maximum penetration depth, and the normal force F_z of tire force is:

$$F_z = k_z(z_0 - z_t + z_b) + d_z(z_0 - z_t + z_b) \quad (1)$$

where: k_z is the normal nonlinear stiffness function of the tire, z_0 is the bridge floor irregularity, z_t is the vertical displacement of the tire, z_b is the displacement of the bridge floor and the contact position of the $tires_x$, and d_z is the tire damping. h is the vertical deformation rate of the tire. The tire longitudinal force F_x is:

$$F_x = \text{sign}(s_x)[uF_z - \frac{uF_z}{s_x}] \quad (2)$$

Tire lateral force F_y is:

$$F_y = uF_z(1-h^2)\text{sign}(s_y) \quad (3)$$

s_y is the lateral creep stiffness, r_t is the tire radius, and the tire righting torque is:

$$M_z = -2uF_z r_t \text{sign}(s_y) \quad (4)$$

Here, we choose a 20-ton vehicle model to investigate how the dynamic response of steel-hybrid composite beam bridges changes as cars cross them at varying speeds. On the assumption that the vehicles are not eccentric and the unevenness grade of the bridge floor is Class A, four distinct operating conditions are described with speeds of 20, 40, 60, and 80 km/h. We examine and evaluate the dynamic response of the central span and the side span at various vehicle speeds.

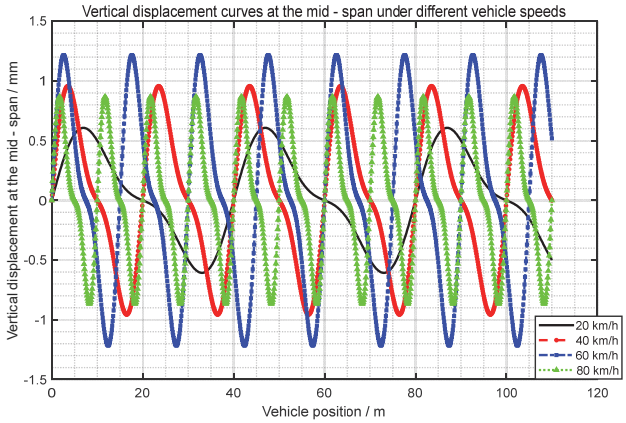

Figure 3 Mid-span vertical displacement of bridge at different speed

The amplitude of the bridge's mid-span vertical displacement fluctuates in a limited range as the vehicle speed rises; its amplitude increases first and subsequently declines, as seen in Fig. 3. At 60 km/h, the vertical displacement amplitude is 2.523 mm at its highest. As seen in Fig. 4, the amplitude of the bridge's mid-span vertical acceleration keeps growing as the vehicle's speed increases. At 80 km/h, the vertical acceleration is at its peak, at 0.107 m/s².

Tab. 4 shows that when the vehicle's speed increases, the mid-span vertical displacement of the side span continues to grow in amplitude, but the mid-span vertical displacement of the span as a whole does not. Differences between the mid-span and edge-span displacement amplitudes are more pronounced in the mid-span versus the edge-span. As a function of vehicle speed, the side span's vertical acceleration is far more variable than the central span's. When examining the dynamic response of a steel-hybrid composite beam bridge at different speeds, it is evident that the amplitudes of vertical displacement and acceleration for each bridge span exhibit very modest changes.

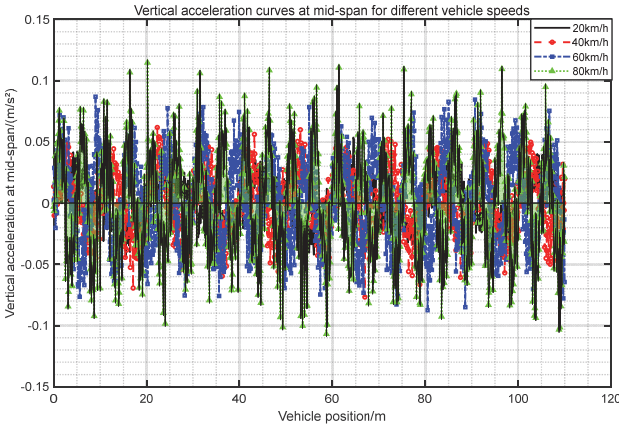

Figure 4 Mid-span vertical acceleration of bridge at different speed

Table 4 Dynamic response amplitudes of each span at different speed

Calculated working condition	20 km/h	40 km/h	60 km/h	80 km/h
Mid-span vertical displacement / mm	2.457	2.478	2.523	2.498
Mid-span vertical acceleration / m/s²	0.038	0.042	0.078	0.107
Mid-span vertical displacement of side span / mm	3.144	3.154	3.275	3.285
Vertical acceleration in span / m/s²	0.046	0.068	0.092	0.125

A vehicle's weight directly impacts the stress on a bridge's structural elements, and it also influences the vibrations felt by those elements to a certain extent. This extract analyses the dynamic response in the middle span and side span of the bridge under different vehicle weights with four different load conditions (10 t, 20 t, 30 t, and 40 t). The study assumes that the vehicle has no eccentricity, travels at 60 km/h, and the deck is grade A. The goal is to study the influence of vehicle weight variation on the vertical dynamic response of steel-hybrid composite girder bridges.

The amplitude of the mid-span vertical displacement of the composite beam bridge shows a noticeable pattern of increasing as the vehicle weight increases from 10 t to 40 t, as shown in Fig. 5. An amplitude of 5.146 mm for mid-span vertical displacement is achieved with a vehicle weight of 40 t. The mid-span vertical acceleration amplitude of the composite beam bridge grows substantially as the vehicle weight increases, as shown in Fig. 6. At 40 tons, the combined beam bridge's mid-span vertical acceleration amplitude reaches 0.156 m/s².

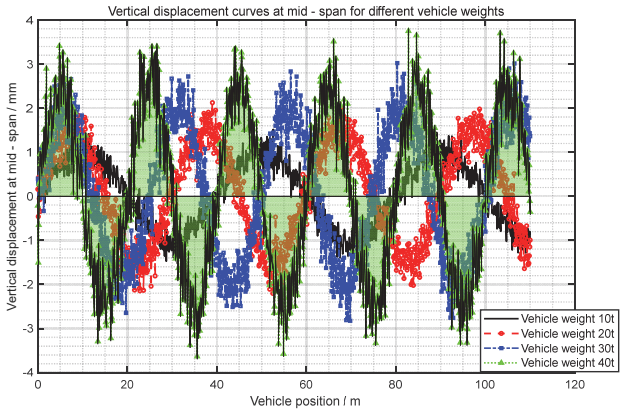

Figure 5 Mid-span vertical displacement of bridge with different vehicle weights

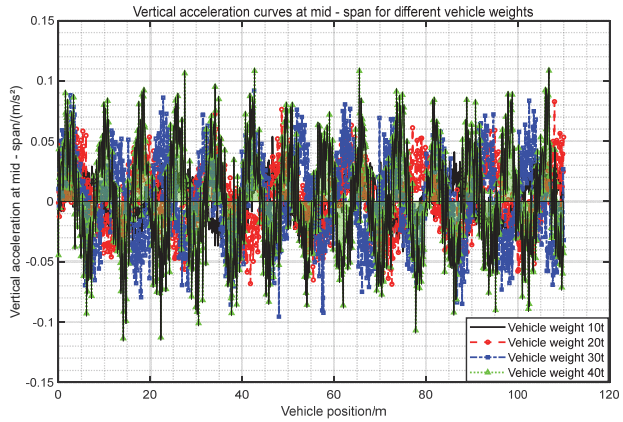

Figure 6. Mid-span vertical acceleration of bridge with different vehicle weights

Table 5 Dynamic response amplitude of each span under different vehicle weights

Calculated working condition	10 t	20 t	30 t	40 t
Mid-span vertical displacement / mm	1.362	2.523	3.784	5.146
Mid-span vertical acceleration / m/s²	0.066	0.078	0.132	0.156
Mid-span vertical displacement of side span / mm	1.619	3.275	4.911	6.544

The vertical maximum response values in the center span and side span of the bridge clearly rise as the vehicle weight increases, as shown in Tab. 5. At 40 metric tons, the mid-span vertical displacement amplitude is 3.778 times that at 10 metric tons. Assuming a vehicle weight of 40 metric tons, the mid-span vertical acceleration amplitude is 2.364% of 10 metric tons. The vertical displacement amplitude of the side span is 4.042 times greater when the vehicle weight is 40 metric tons than when the vehicle weight is 10 metric tons. By a factor of 2.479, the vertical acceleration amplitude of the side span increases from 10t to 40t, a significant increase. The dynamic response of the steel-composite beam bridge is significantly affected by the vehicle's weight. As the vehicle's weight increases, the vibration effect of the coupling dynamic system between the bridge and the vehicle becomes more pronounced, potentially jeopardizing the bridge's safety. Consequently, this factor requires sufficient attention.

Cars traveling on bridge decks can experience excessive vibration due to deck irregularities, which in turn increases the force of impacts with the pavement of the bridge decks. This, in turn, can harm cars and compromise the bridge's traffic safety. The dynamic response of the bridge is significantly impacted by the irregularity of the bridge floor, which is the primary initial excitation source in the vehicle-bridge coupling vibration system. Fig. 7 shows that when the deck irregularity grade goes from class A to class C, the amplitude of the mid-span vertical displacement of the bridge and the fluctuation degree of the mid-span vertical displacement curve both go up substantially. For bridges with a class C deck irregularity grade, the maximum amplitude of the mid-span vertical displacement is 3.242 mm. The magnitude of mid-span vertical acceleration grows substantially when the condition of the bridge floor deteriorates, as seen in Fig. 8. In a deck with an unevenness grade of C, the mid-span vertical acceleration amplitude can reach 0.272 m/s².

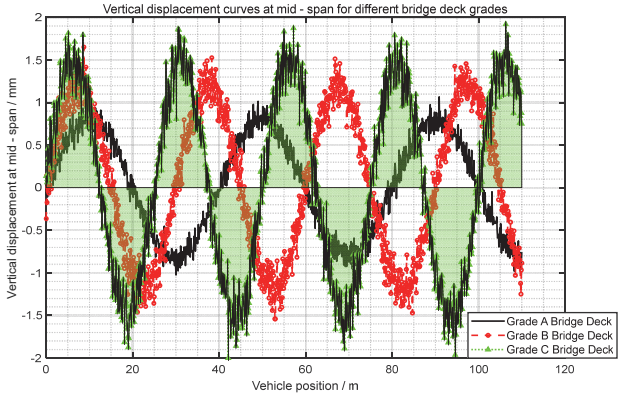

Figure 7 Mid-span vertical displacement of bridges with different deck irregularity levels

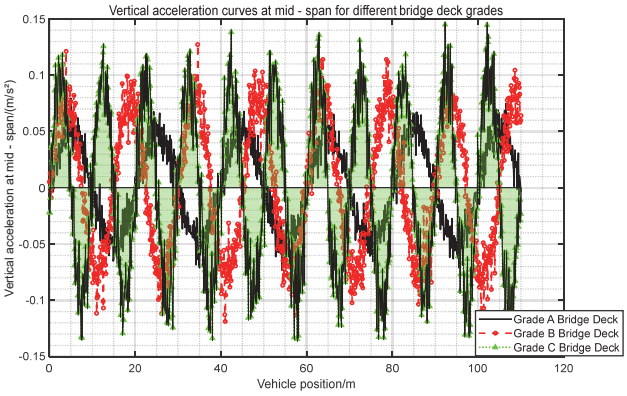

Figure 8 Mid-span vertical acceleration of Bridges with different deck irregularity levels

Table 6 Dynamic response amplitude of each span under different deck irregularity levels

Calculated working condition	Rank A	Rank B	Rank C
Mid-span vertical displacement / mm	2.523	2.843	3.242
Mid-span vertical acceleration / m/s²	0.078	0.123	0.272
Mid-span vertical displacement of side span / mm	3.275	3.398	4.115
Vertical acceleration in span / m/s²	0.092	0.166	0.323

According to Tab. 6, Class A bridges have mid-span vertical displacement amplitudes that are 1.13 times larger than Class B bridges and 1.28 times larger than Class C bridges when the deck is uneven. Class A bridges have mid-span vertical displacement amplitudes that are 1.04

times larger than Class C bridges and 1.26 times larger than Class A bridges under uneven deck conditions. As the deck irregularity grade increases, the vibration of the bridge becomes more severe, and the largest displacement of the bridge is observed in the middle of the side span, in comparison to the vertical displacement in the span and side span. Class B and Class C bridges, when subjected to an uneven deck, have mid-span vertical acceleration amplitudes that are 1.58 and 3.49 times larger than the comparable amplitudes of class A, respectively. Under Class A's uneven deck, the vertical acceleration amplitude of the bridge side span is 1.80 times larger than Class C's, and 3.51 times more than Class A's comparable amplitude. As the degree of deck irregularity increases, the vertical acceleration values in the bridge's middle and side spans grow substantially. A key aspect impacting the coupling vibration of a steel-composite beam bridge is deck irregularity, and it is clear that a decline in deck flatness would greatly increase the influence of vibration on the vehicle-bridge coupling.

3.3 Analysis of Influencing Factors of Vehicle Dynamic Response

Car ride quality and security are impacted by vibrations in axle couplings. When a car is kept firmly in its lane, its vibration law can be somewhat reflected in its changes in vertical displacement and acceleration. In this part, as criteria to define distinct working circumstances, we utilized four speeds of 20 km/h, 40 km/h, 60 km/h, and 80 km/h to evaluate the influence of variations in vehicle speed on vehicle dynamic response. Assuming the vehicle was eccentrically free and the bridge floor irregularity grade was A, the vehicle load was 20 t. The analysis focuses on the vertical acceleration and displacement of the vehicle's centroid as it crosses the bridge at various speeds.

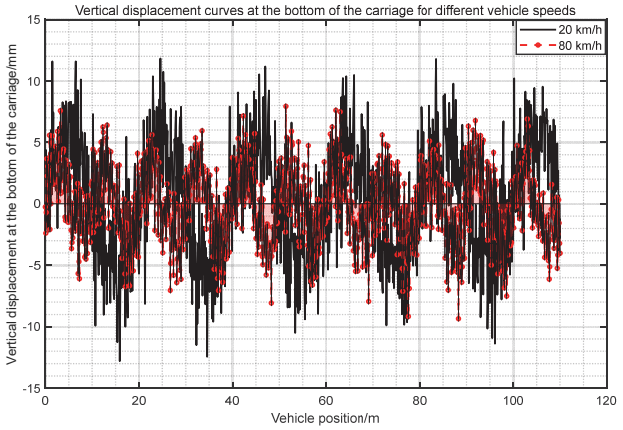

Figure 9 Vertical displacement of vehicles at different speed

Figs. 9 and 10, and Tab. 7 show that the vertical displacement amplitude of the vehicle centroid does not change much as the speed of the vehicle increases. The vertical displacement amplitude of the vehicle centroid is 15.238 mm at a speed of 40 km/h and 15.642 mm at 80 km/h. No significant change is seen between these two speeds. As speed rises, the centroid of the vehicle experiences a linear increase in vertical acceleration. At 80 km/h, the centroid's vertical acceleration amplitude reaches a maximum of 1.225 m/s². The centroid's vertical acceleration is 1.04 times, 1.08 times, and 1.11 times that of the comparable value at 20 km/h when the vehicle speed is 40, 60, and 80 km/h, respectively. It is clear that the vibration caused by a change in vehicle speed is negligible.

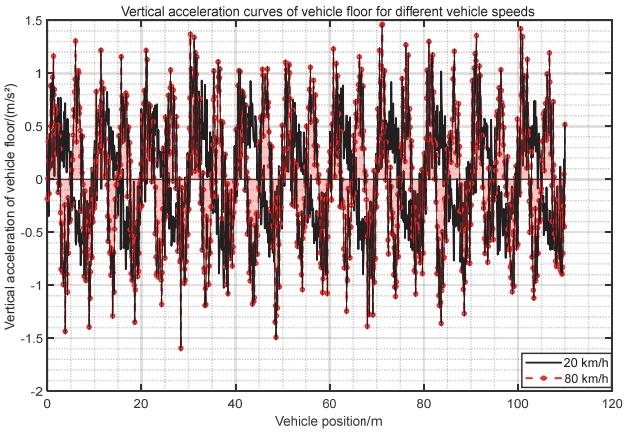

Figure 10 Vertical acceleration of vehicles at different speed

Table 7 Dynamic response amplitude of vehicle centroid at different speeds

Calculated working condition	20 km/h	40 km/h	60 km/h	80 km/h
Vertical displacement of vehicle centroid / mm	15.346	15.238	15.413	15.642

Because of the link between the vehicle and the bridge, any vehicle traveling on the bridge deck will experience vertical vibration response as a result of both the bridge's unevenness and the deck's deformation. This section provides various operating circumstances with three levels of deck irregularity, Class A, Class B, and Class C, respectively, in order to explore the effects of deck deformation and irregularity on the dynamic response of vehicles. Assuming the car is not eccentric and is traveling at 60 km/h, the weight on the vehicle is 20 t. When cars travel over various uneven decks, we measure and compare the centroid's vertical displacement and acceleration.

As can be seen from Fig. 11, Fig. 12 and Tab. 8, the vertical displacement amplitude of vehicle centroid increased by 2.19 times from 15.436 mm to 33.881 mm in the process of bridge deck irregularity changing from good to bad. With the increase of deck irregularity, the vertical acceleration amplitude of vehicle centroid continues to increase. The vertical acceleration of the vehicle centroid is 1.53 times and 2.70 times of the corresponding value of the A-class bridge deck when the deck irregularity level is B and C, respectively. In general, as the deck irregularity worsens, the greater the vertical dynamic response of vehicles, the deck irregularity significantly affects the dynamic response of vehicles.

Table 8 Dynamic response amplitude of vehicle centroid under different deck irregularity levels

Calculated working condition	Rank A	Rank B	Rank C
Vertical displacement of vehicle centroid / mm	15.436	19.512	33.881
Vertical acceleration of vehicle centroid / m/s²	1.192	1.824	3.217

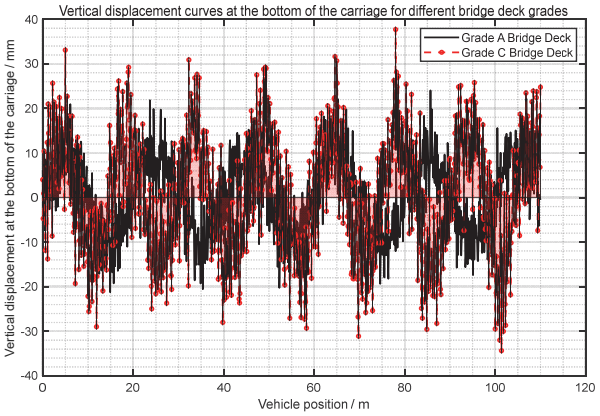

Figure 11 Vertical displacement of vehicles at different levels of deck irregularity

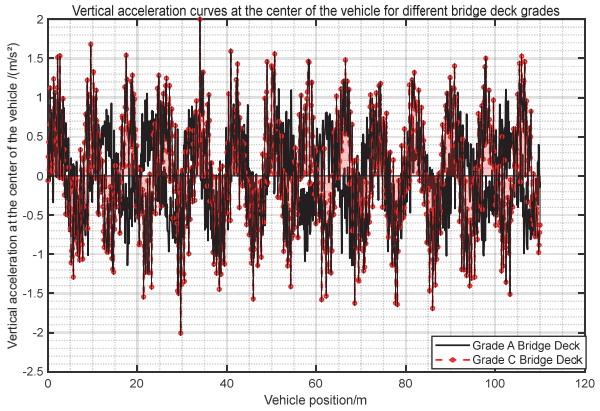

Figure 12 Vertical acceleration of vehicles at different levels of bridge deck irregularity

4 COMPARATIVE STUDY ON IMPACT COEFFICIENT OF CURVED STEEL-HYBRID CONTINUOUS BEAM BRIDGE

4.1 Finite Element Model of Bridge

We use four different-section continuous beam bridges as our study objects, and we build our bridge model from the blueprints. There are four types of continuous girder bridges: box girder bridges made of steel-mixed composite, I-beam composite, tiny box girder bridges made of prestressed concrete, and T girder bridges made of prestressed concrete. On the highway, they are all rated for Class I loads. The dimensions of the bridge are 3 × 40 m for the span, 1.7 m, 2.4 m, 2.0 m, and 2.5 m for the beam heights, and 13 m, 12.25 m, 12 m, and 12 m for the deck widths. Paving on the bridge deck is 100 mm thick and made of asphalt concrete. The fundamental bridge specifications are displayed in Tab. 9.

Table 9 Bridge model parameters

Bridge type	Short	Span combination / m	Base frequency / Hz	u gauge value
Steel-composite box girder bridge	SCCB120	3 × 40	2.24	0.127
Steel-composite I-beam bridge	SCCI120	3 × 40	2.56	0.150
Small box girder bridge	B120	3 × 40	2.30	0.131
T-beam bridge	T120	3 × 40	2.91	0.173

Table 10 Natural vibration frequency of bridge model

Order	SCCB120		SCCI120		B120		T120	
	Frequency / Hz	Mode characteristics	Frequency / Hz	Mode characteristics	Frequency / Hz	Mode characteristics	Frequency / Hz	Mode characteristics
1	2.24	Vertical bend	1.55	Transverse vibration	2.30	Vertical bend	2.91	Vertical bend
2	2 2.82	Vertical bend	1.78	Transverse vibration	2.97	Vertical bend	3.28	twist
3	3 3.90	Vertical bend	2.56	Vertical bend	4.24	Vertical bend	3.76	Vertical bend
4	4 6.25	twist	3.11	Cross bend + twist	5.42	twist	3.85	twist
5	5 6.52	twist	3.27	Vertical bend	5.78	twist	4.93	twist

In order to determine the frequency of the continuous beam bridge and to extract the first five vibration frequencies of the bridge structure, modal analysis was performed using the finite element program ABAQUS. The results are displayed in Tab. 10.

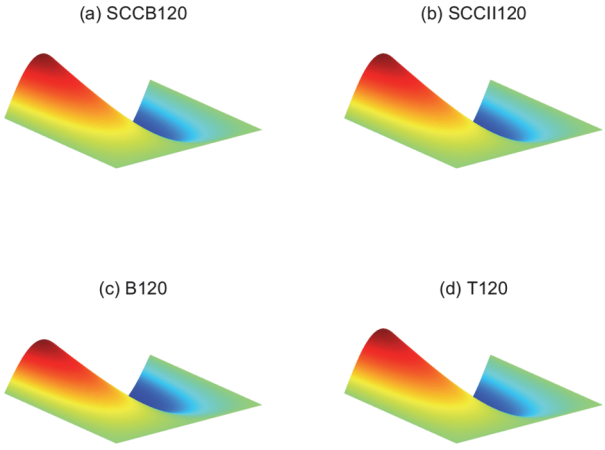

Figure 13 Vibration mode of continuous beam bridge

In Fig. 13, we can see the initial modes of vibration caused by vertical bending in four continuous beam bridges. Vibration in every direction was symmetrical and bowed vertically.

4.2 Comparative Study on Impact Coefficient of Steel-Hybrid Continuous Beam Bridge

It is generally believed that road roughness [17] is a stable and uniform Gaussian random process with zero mean of all states, which is usually represented by power spectral density:

$$G_d(n) = G_d(n_0)/(n/n_0)^{-w} \tag{5}$$

Using Fourier transform n_k to generate road roughness:

$$\gamma(X) = \sum_{k=1}^{N} \sqrt{2\varphi n_k} \cos(2\pi n_k X) \tag{6}$$

Considering the excitation effect of class A, Class B and Class C deck irregularity, the influence law of deck irregularity on 4 continuous beam Bridges is analyzed. A total of 5 vehicle speed conditions were set under the same level of bridge deck, and 10 times of vehicle-bridge interaction analysis considering random samples of bridge deck irregularity were carried out for each condition. A total of 50 random samples of impact coefficient are generated under each deck grade. The impact coefficient of deflection in the middle section of four continuous beam Bridges is averaged, and the standard deviation of the sample population of 50 impact coefficients is calculated. Fig. 14 shows the curve of mid-span impact coefficient changing with bridge floor irregularity, and the vertical error bar is used to represent the magnitude of the corresponding standard deviation.

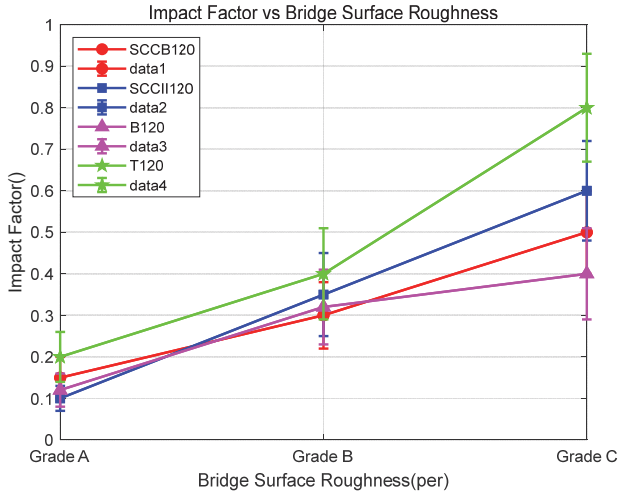

Figure 14 Influence of deck irregularity on impact coefficient

As the roughness level of a bridge deck rises from class A to class C, the condition of the deck gets worse with time. Consistent with the findings of other researchers, Fig. 13's curve demonstrates that the impact coefficient of a continuous beam bridge grows exponentially with increasing bridge surface roughness. A deck's impact coefficient is greatly affected by its degradation. A nonlinear growth trend is observed in the impact coefficient when the amount of bridge floor irregularity increases from class A to class C. The impact coefficient and slope of the curve both increase as a result. Lowering the bridge deck grade causes a rise of 0.154 and 0.238 for SCCB120, 0.172 and 0.209 for SCCI120, 0.168 and 0.181 for B120, and 0.251 and 0.365 for T120, correspondingly. The T120 impact coefficient of the prestressed concrete continuous T-beam bridge reaches 0.365 when the deck grade is dropped from class B to class C, which is the highest value.

By observing the height of vertical error bar in Fig. 14, it can be found that the random sample standard deviation of impact coefficient of continuous beam bridge significantly increases with the decrease of deck grade. With the increase of bridge surface roughness, the dispersion degree of impact coefficient will increase. Among the four continuous beam Bridges with the same span combination under the same deck irregularity excitation, the standard deviation of the impact coefficient of the continuous T-beam bridge T120 under three different deck grades is significantly greater than that of the other three Bridges, while the impact coefficient of the two steel-mixed composite beam Bridges and the prestressed concrete small box girder Bridges shows a relatively consistent law, and the values of the three are consistent with the curves.

The ANSYS (Large-scale general finite element analysis (FEA) software) bridge model is imported into the dynamics software UM (User Manual) to complete the simulation of vehicle-bridge coupling, adjust the vehicle trajectory so that it can drive in different lanes, set the vehicle speed, vehicle weight and bridge floor irregularity and other working conditions in UM, select the measuring point and the displacement and tangential stress required to calculate, complete the vehicle driving on the bridge under different working conditions, and then directly generate the no of each measuring point Displacement and tangential stress response curve with driving distance under the same working condition.

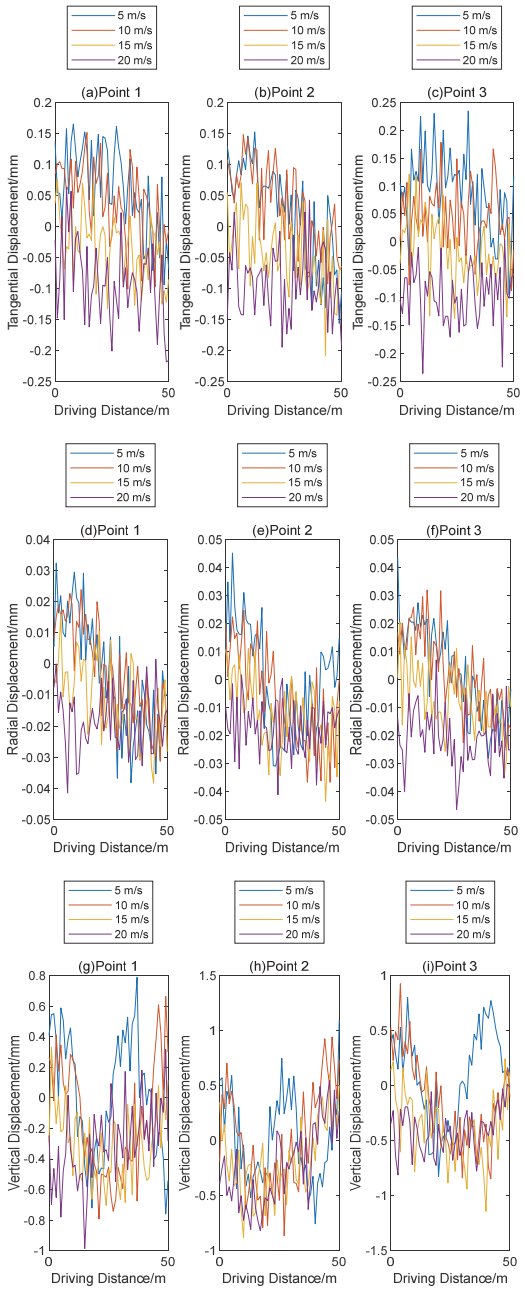

Figure 15 Displacement response of bottom plate at different speed

The positive direction of tangential displacement is the direction of vehicle travel. As can be seen from Fig. 15a-c Tangential displacement of measuring points, vehicle speed has little influence on tangential displacement of measuring points in mid-span. At different speeds, the tangential displacement response curves of the three measuring points are the same, and the peak values are basically the same. When the vehicle is traveling in the first span, the displacement direction of the measuring point is opposite to the direction of the vehicle. When the vehicle is traveling in the middle span, the measuring point moves in the direction of the vehicle. When the vehicle is located in the middle span, the displacement of the measuring point is maximum. When the vehicle is located in the third span, the displacement of the measuring point is small.

The positive direction of radial displacement refers to the outside direction of the curve. It can be seen from Fig. 15d-f radial displacement of measuring points that the driving speed has a certain influence on the mid-span radial displacement, and the greater the driving speed, the greater the radial displacement of measuring points. When the vehicle is driving on the side span, the measuring point moves to the inside of the curve. When the vehicle is driving in the mid-span, the measuring point moves to the outside of the curve.

The positive direction of vertical displacement is vertical upward. The following conclusions can be drawn from the vertical displacement response of measuring points in Fig. 15g-i: Vehicle speed has little influence on the vertical displacement of measuring points in the middle span of the bridge, and the trend of vertical displacement response curve is basically the same under different vehicle speeds. Under different speed, the peak value of the response curve is different, that is, the dynamic vibration amplitude is different, and the amplitude is not simply positively or negatively correlated with the speed.

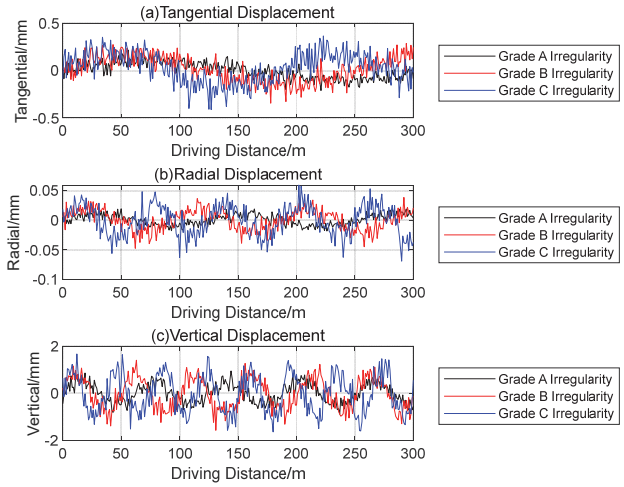

Figure 16 Displacement response of floor under excitation of different deck irregularity

Fig. 16 shows the displacement response curve of the floor under different irregularity conditions. It can be seen that with the increase of irregularity grade, the three displacement responses are gradually intense, and the tangential displacement response and vertical displacement response fluctuate more obviously. When the bridge deck level is C, the fluctuation of the three stress response curves is obviously enhanced when the vehicle travels to the third span, that is, the resonance of the coupling system of the uneven alighting bridge occurs to a certain extent.

5 CONCLUSION

An ABAQUS finite element model of the bridge and vehicle is constructed in accordance with the fundamental theory of vibration coupling between the two. The numerical study of the vibration of the vehicle-bridge coupling is carried out using the ABAQUS single environment, taking into account the role of the bridge floor's irregularities. Plane half-car, two-axle vehicle, and I-steel composite beam bridge coupling vibration analyses are performed. The findings demonstrate the impressive accuracy of the suggested approach. This study examines four 3 × 40 m continuous beam bridges and the laws of effect for vehicle speed, imbalance of the bridge deck, frequency of the bridge, and impact coefficient of the main beam cross section. Not only can continuous beam bridges achieve impact coefficient properties comparable to simple supported beam bridges, but they also show a reduced impact coefficient compared to simple supported beam bridges of the same span. While the impact coefficients of pre-layered concrete continuous small box bridges, steel-mixed I composite continuous box bridges, and prestressed concrete continuous T-beam bridges are all generally constant, the impact coefficient of a single prestressed concrete continuous T-beam bridge is significantly bigger. Both the vehicle and the steel-mixed composite beam bridge see a dramatic increase in dynamic reactivity as the deck quality worsens. Decks with a Class A rating are safe for both pedestrians and drivers since their impact coefficients are lower than the industry norm. A deck grade of B ensures that both pedestrians and drivers are comfortable, as the impact coefficient is near the standard value. The impact coefficient is significantly more than the normal value when the bridge deck slope is C, and while pedestrian comfort fulfills the criteria, driving comfort does not. A vehicle-bridge coupling vibration is greatly affected by the bridge deck's unevenness. Management staff should prioritize the upkeep of the bridge deck pavement as part of the daily management of the bridge. This paper has not yet taken into account the changes in bridge structure parameters among the influencing factors of vehicle-bridge coupling vibration, which is also the focus of the next research.

Acknowledgments

This work was supported by the Key Projects of Natural Science Research Programs of Universities in Anhui Province, (No. 2022AH051094); Chuzhou University Scientific Research Startup Fund Project, (No.

2022qd019); Key Research Project of Natural Science in Colleges and Universities of Anhui Province, (No. 2024AH051404).

6 REFERENCES

[1] Cao, H., Lu, Y., & Chen, D. (2024). Analysis of Vehicle-Bridge Coupling Vibration Characteristics of Curved Girder Bridges. *Applied Sciences-Basel*, *14*(5), 17-31. https://doi.org/10.3390/app14052021

[2] Eng, Y., Ma, W., & Tan, Y. (2024). Approach of Dynamic Tracking and Counting for Obscured Citrus in Smart Orchard Based on Machine Vision. *Applied Sciences-Basel*, *14*(3), 14-36. https://doi.org/10.3390/app14031136

[3] Zheng, Y., Lu, C., & Huang, X. (2024). Impact of Variable Parameters of Expansion Joints and Bearing Supports on the Vehicle-Induced Vibration of Curved Girder Bridges. *Buildings (2075-5309)*, *14*(1), 293-302. https://doi.org/10.3390/buildings14010293

[4] Sadik, S., Awall, M. R., & Hasan, M. (2023). Natural vibration characteristics of horizontally curved steel twin I girder bridge. *AIP Conference Proceedings*, *2713*(1), 9-31. https://doi.org/10.1063/5.0130031

[5] Aribas, U. N. (2024). Bi-directional higher-order shear deformable mixed finite element formulation including couple effects for stresses of functionally graded curved 3d beams. *Journal of the Brazilian Society of Mechanical Sciences and Engineering*, *2024*(11), 46-71. https://doi.org/10.1007/s40430-024-05211-3

[6] Yin, C., Xiao, Y., & Zhang, Z. (2024). Design framework for phononic crystals based on compression-twist coupling structures with curved beams.*International Journal of Mechanical Sciences*, *266*(2), 19-39. https://doi.org/10.1016/j.ijmecsci.2023.108920

[7] Qi, W., Ye, X., & Wang, X. (2025).Reverse design and application of phononic crystals based on deep learning. *Journal of Physics D: Applied Physics*, *58*(4), 16-33. https://doi.org/10.1088/1361-6463/ad8933

[8] Zhi, Yuan, C., Xin, L., & Cheng, S. (2024). Numerical study on the effect of distortion of S-duct on flow field and performance of a full annulus transonic fan. *International Journal of Turbo and Jet Engines*, *2024*(2), 41-68. https://doi.org/10.1515/tjj-2023-0019

[9] Lu, B., Song, Y., & Liu, Z. (2025). Evolution Analysis of Three-Dimensional Wheel Polygonal Wear for Electric Locomotives Considering the Effect of Interharmonics. *Vehicular Technology, IEEE Transactions*, *74*(2), 2443-2457. https://doi.org/10.1109/TVT.2024.3474035

[10] Darvishi, F. & Rahmani, O. (2023).Calibration of nonlocal generalized helical beam model for free vibration analysis of coiled carbon nanotubes via molecular dynamics simulations. *Mechanics of Advanced Materials & Structures*, *30*(8), 26-39. https://doi.org/10.1080/15376494.2022.2038739

[11] Hu, W., Zhang, Z., & Shi, J. (2024). Refined Analysis of Spatial Three-Curved Steel Box Girder Bridge and Temperature Stress Prediction Based on WOA-BPNN. *Buildings*, *14*(2), 18-35. https://doi.org/10.3390/buildings14020415

[12] Xu, H., Xiao, X., & Liu, X. (2024). Study on the influence of car-body flexibility on passengers' ride comfort. *Vehicle System Dynamics*, *62*(8), 39-58. https://doi.org/10.1080/00423114.2023.2271585

[13] Scala, A, L., Liwa-Wieczorek, K., & Rizzo, F. (2024). Flexible Polyurethane Adhesives: Predictive Numerical Model Calibration through Experimental Testing at Elevated Temperature. *Applied Sciences-Basel*, *14*(5), 18-43. https://doi.org/10.3390/app14051943

[14] Reyes, S. I., Vassiliou, M. F., & Konstantinidis, D. (2024). Experimental characterization and constitutive modeling of thermoplastic polyurethane under complex uniaxial loading. *Journal of the Mechanics and Physics of Solids*, *186*(May), 105582.1-105582.24. https://doi.org/10.1016/j.jmps.2024.105582

[15] Wang, X., Wei, K., & Ma, Q. (2024). Research on fastener lateral nonlinear stiffness characteristics and its impact on wheel-rail stick-slip vibration. *Nonlinear Dynamics*, *112*(19), 99901-99916. https://doi.org/10.1007/s11071-024-09990-1

[16] Zhang, X., Li, J., & He, H. (2025). Study of Fire Plume Behavior and Maximum Ceiling Temperature Rise in a Curved Tunnel Driven by the Coupling of Blockage Effect and Longitudinal Ventilation. *Fire (2571-6255)*, *8*(1), 1009-1023. https://doi.org/10.3390/fire8010009

[17] Yin, C., Xiao, Y., & Zhang, Z. (2024). Design framework for phononic crystals based on compression-twist coupling structures with curved beams. *International Journal of Mechanical Sciences*, 266-278. https://doi.org/10.1016/j.ijmecsci.2023.108920

[18] Tian, Z., Yue, L., & Qi, C. (2024). Effect of magnetic field excitation and sinusoidal curved cavity coupling on heat transfer enhancement and entropy generation of nanofluids. *Journal of Thermal Analysis & Calorimetry*, *149*(22), 13596-13601. https://doi.org/10.1007/s10973-024-13596-5

[19] Sun, H., Li, C., & Han, X. (2025). Study on the multifield coupling mechanism in laser cladding of 316L under different elevation angles of the laser head. *Journal of Laser Applications*, 37(1), 12020-12035. https://doi.org/10.2351/7.0001672

[20] Huang, W. Y., Hwu, C., & Hsu, C. W. (2024). Bending-extension coupling analysis of shear deformable laminated composite curved beams with non-uniform thickness. *Engineering Structures*, 305-328. https://doi.org/10.1016/j.engstruct.2024.117696

[21] Senkoua, Y., Ngak, F. P. E., & Meuyou, H. H. (2024). Numerical Investigation of the Vibroacoustic Behavior of Carbon Nanotube Reinforced Doubly-Curved Multilayer Composite Shells. *Mechanics of Solids*, *59*(8), 4003-4026. https://doi.org/10.1134/S0025654424605093

[22] You, R., Ren, L., & Li, Y. H. (2023). Deformation estimation of plane-curved structures using the NURBS-based inverse finite element method. *Structural engineering and mechanics*, *88*(1), 83-94. https://doi.org/10.12989/sem.2023.88.1.083

[23] Linlin, S., Mingyang, W., & Xueming, Z. (2025). Mechanical Performance Analysis of Long Span High-speed Railway Station Roofs Considering the Coupling Effect of Low Temperature and Extreme Snow Load. *Railway Standard Design*, *69*(1), 6-21. https://doi.org/10.13238/j.issn.1004-2954.202306080006

[24] Wang, C. S., Wang, Y. Z., & Shu, C. D. (2024). Digital simulation of distortion-induced fatigue in steel bridges with different geometrical configurations. *Journal of Constructional Steel Research*, *216*(May), 1.1-1.16. https://doi.org/10.1016/j.jcsr.2024.108613

[25] Wang, C., Sui, J., & Wang, X. (2025). Vortex flow properties and enhanced heat transfer analysis of ferrofluid in a curved pipe under the coupling of magnetic field force and centrifugal force. *Journal of Mechanical Science & Technology*, *39*(1), 24-37. https://doi.org/10.1007/s12206-024-1237-z

[26] Lv, X., Zhang, Y., & Shi, Q. (2024). Multibeam Cylindrical Conformal Array in the Presence of Enhanced Mutual Coupling. *Electronics*, *13*(2), 17-37. https://doi.org/10.3390/electronics13020373

Contact information:

Hao QU
(Corresponding author)
School of Civil Engineering and Architecture,
Chuzhou University, Chuzhou 239000, Anhui, China
Anhui Provincial International Joint Research Center of Data Diagnosis and Smart Maintenance on Bridge Structures,
Chuzhou 239000, Anhui, China
E-mail: quhao1987@foxmail.com

Yufeng LIU
School of Civil Engineering and Architecture,
Chuzhou University, Chuzhou 239000, Anhui, China
Anhui Provincial International Joint Research Center of Data Diagnosis and Smart Maintenance on Bridge Structures,
Chuzhou 239000, Anhui, China

Shuigen HU
School of Civil Engineering and Architecture,
Chuzhou University, Chuzhou 239000, Anhui, China
Anhui Provincial International Joint Research Center of Data Diagnosis and Smart Maintenance on Bridge Structures,
Chuzhou 239000, Anhui, China